Supporting Information

Anomalous Manganese Activation of a Pyrophosphate Cathode in Sodium Ion Batteries: A Combined Experimental and Theoretical Study

Chan Sun Park,[†,∥] Heejin Kim,[†,∥] Rana A. Shakoor, [§,∥] Eunjeong Yang,[†] Soo Yeon Lim,[†] Ramazan Kahraman,[§] Yousung Jung,*[,†, ‡] and Jang Wook Choi*[,†, ‡]

[†]Graduate School of EEWS (WCU) and [‡]KAIST Institute NanoCentury, Korea Advanced Institute of Science and Technology (KAIST), Yuseong-gu, Daejeon 305-701, Republic of Korea

[§]Department of Chemical Engineering, College of Engineering, Qatar University 2713, Doha, Qatar

Experimental section

Synthesis. We synthesized $Na_2MnP_2O_7$ by conventional solid state reactions under argon flow. The compound was prepared by thoroughly mixing the stoichiometric amounts of Na_2CO_3 (≥99.5 %, Sigma-Aldrich), $(NH_4)_2HPO_4$ (≥99.9 %, Sigma-Aldrich) and MnO_2 (≥99.9 %, Alpa-Aesar). The powders were pelletized and annealed at 350 °C for 3 hrs in argon atmosphere. The pelletized powders were cooled to room temperature and were then ground. The ground powders were re-pelletized and then sintered at 500 °C for 9 hrs in argon atmosphere. The as-synthesized samples were carbon-coated through a dry ball milling process at a speed of 500 rpm for 24 hrs (the ratio of the active material to Super P is 8:2 in weight). After the carbon coating process, the carbon coated powder was re-pelletized and annealed once again at 500 °C for 9 hrs under argon atmosphere to restore the crystallinity. In order to prepare the samples for Ex-situ XRD characterization, $Na_2MnP_2O_7$ was electrochemically oxidized to various potentials at a C/10 rate.

XRD and SEM Characterization. A multi-purpose attachment X-ray high power diffractometer (RIGAKU, D/MAX-2500, Tokyo, Japan) equipped with Cu Kα radiation was used for evaluating the crystal structures of the synthesized materials. The XRD pattern indexing of the as-synthesized material was performed using the Jana2006 software. The morphological images of the as-synthesized material were obtained by field emission-scanning electron microscopy (FE-SEM, Philips, XL30 FEG, Eindhoven, Netherlands) at 10 kV accelerating voltages.

Electrochemical tests. For electrode fabrication, slurry was first prepared by mixing carbon coated active material (75 wt %), Super P (15 wt %) and polyvinylidene fluoride (PVDF) (10 wt %) and dissolving the mixture in N-methyl-2-pyrrolidone (NMP). The slurry was cast on aluminum foil, and NMP was evaporated at 70 °C for 24 hrs inside a vacuum oven. The mass loading of the active material was ~ 1mg/cm^2 for all of the samples. 2032 type coin cells were prepared by assembling the active electrodes, sodium thin disks, separators (Celgard 2400) soaked with 1M sodium perchlorate ($NaClO_4$) in propylene carbonate (PC) in an argon filled glove box. The charge and discharge profiles of $Na_2MnP_2O_7$ were obtained by using a battery cycler (WBCS 3000, Wonatech Co.) at room temperature. In order to prepare the samples for Ex-situ XRD characterization, $Na_2MnP_2O_7$ was electrochemically oxidized to various potentials at a C/10 rate. Once the target potentials were reached, the potential was on hold for 7 hrs to ensure complete reaction.

Compositional analysis. The compositions of the pristine and electrochemically oxidized samples were evaluated by inductive coupled plasma mass spectroscopy (ICP-MS, HP 4500) and the results are tabulated in Table S1 and S2.

Density functional theory (DFT) calculations

Calculation details. We performed spin-polarized DFT calculations by using Perdew-Burke-Ernzerhof (PBE) exchange-correlation functional[25] and projector-augmented wave (PAW) method[26] as implemented in the Vienna Ab-initio Simulation Package (VASP).[27] We addressed the self-interaction energy by using Hubbard U-corrections (U = 5.5 eV for Mn) in the rotationally invariant form for the total energy and geometry calculations.[28,29] The calculated ground state energies for different spin orderings were slightly different (less than 10 meV/f.u.) according to the sodium composition, hence all calculations were performed in a high-spin ferromagnetic ordering for consistency. We used a periodic cell of around 13.3 Å × 9.6 Å × 11.2 Å containing 8 formula units of $Na_2MnP_2O_7$. A plane wave basis set with an energy cutoff of 500 eV and 2 × 2 × 2 Monkhorst-Pack *k*-point mesh was sampled for all calculations to give well converged energy values.[30] All crystal structures were visualized using the VESTA software.[31]

Voltage calculations. For the formation energy calculations, the 30 lowest electrostatic energy configurations determined from the Ewald summation[32, 33] were used as an input for fully-relaxed geometry optimizations at each composition. Additional sodium orderings adopted from the previous $Na_2FeP_2O_7$ calculations were also used.[12]

Since the free energy change (ΔG_r) can be approximated by internal energy change (ΔE_r) for solids, the average voltage can be expressed as[34]

$$\bar{V}(x) = -\frac{\Delta G_r}{(x_2-x_1)F} \approx -\frac{\Delta E_r}{(x_2-x_1)F} = -\frac{E^{x_2}-E^{x_1}-(x_2-x_1)E^{Li}}{(x_2-x_1)F} \quad ,$$

where E^x and E^{Li} are the calculated total energies of host material of composition x and lithium, respectively, and F is the Faraday constant. In this work, we used the ensemble average of the total energy at each composition, $\langle E^x \rangle$, instead of a minimum energy alone.[12]

$$\langle E^x \rangle = \sum_i E_i^x P_i^x \quad ,$$

where E_i^x is the total energy of the given configuration and P_i^x is the probability of seeing that particular configuration given by

$$P_i^x = e^{-E_i/kT} / \sum_i e^{-E_i/kT}.$$

Above sampling and ensemble average approach is applicable to any property, such as energy, site occupancy, lattice parameter, oxidation state, and simulated XRD pattern.

XRD pattern calculations. For the simulated XRD patterns, we stretched calculated patterns by 1% along the 2-theta axis to address inherent errors originated from a general overestimation of lattice parameters in the generalized gradient approximation (GGA) methods. We also used ensemble average for the calculated XRD patterns.

Atomic displacements and bond length changes. The atomic displacements and bond length changes were calculated from the most stable structures at charged and discharged states. The validity of the calculated structures was confirmed from the simulated XRD patterns. To obtain the absolute atomic positions for the displacements calculation, we used averaged lattice parameters for the initial and final structures. The origin was aligned by using the center of mass for each structure. The errors from these adjustments are negligible (~ 0.01 Å) compared to the atomic displacements.

Table S1. ICP compositional analysis of as-synthesized $Na_2MnP_2O_7$ sample.

Element	Weight [%]	Number of Moles	Atomic [%]	Atomic Ratio
Na	0.6682	0.029052	0.397162	2.06
Mn	0.7755	0.0141	0.192757	1.00
P	0.9299	0.029997	0.41008	2.13

Table S2. ICP compositional analysis of electrochemically oxidized $Na_2MnP_2O_7$.

Element	Weight [%]	Number of Moles	Atomic [%]	Atomic Ratio
Na	0.9852	0.042835	0.253992	1.08
Mn	2.1859	0.039744	0.235663	1.00
P	2.6681	0.086068	0.510345	2.17

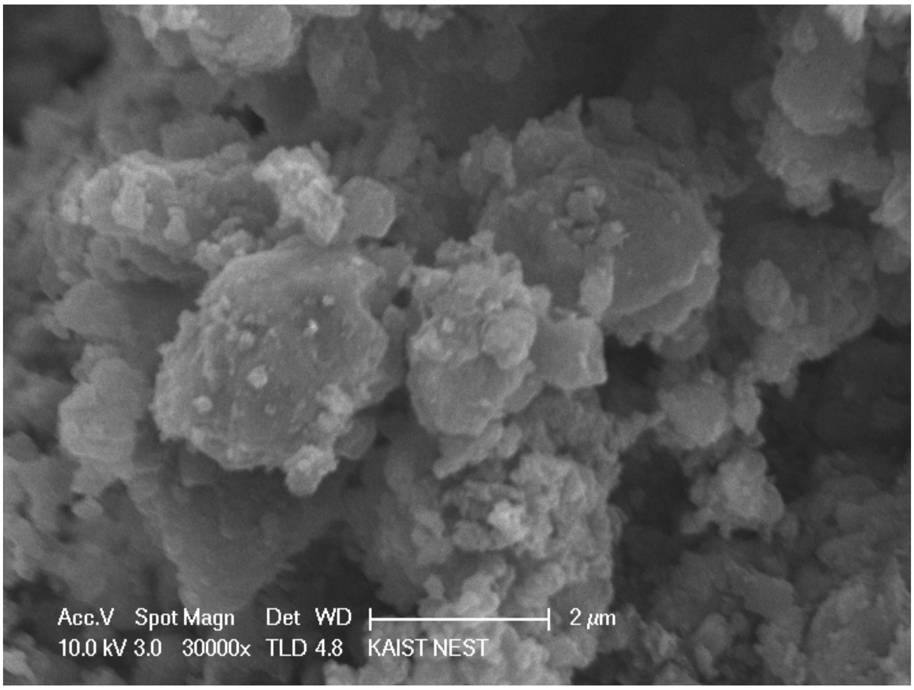

Figure S1. An SEM image of the carbon coated sample.

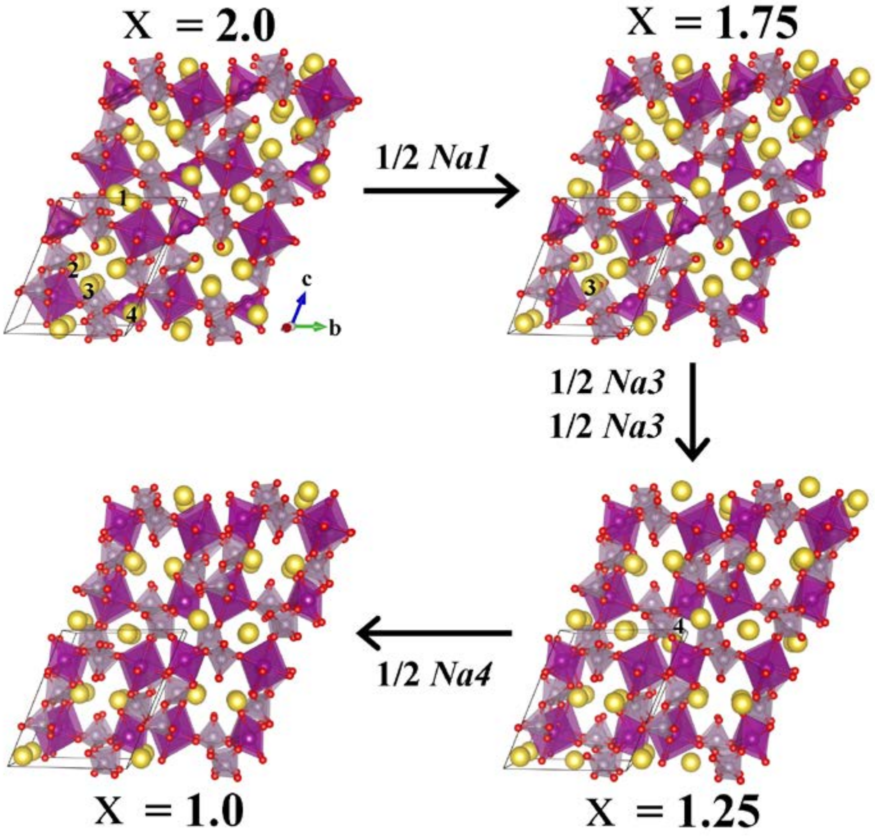

Figure S2. The most probable sodium orderings, i. e., the minimum energy structures at each composition of $Na_xMnP_2O_7$. The purple, grey, red, and yellow spheres present Mn, P, O, and Na atoms, respectively. The Na ions in a half of *Na1* site are firstly extracted followed by all of *Na3* site and a half of *Na4* site are extracted.

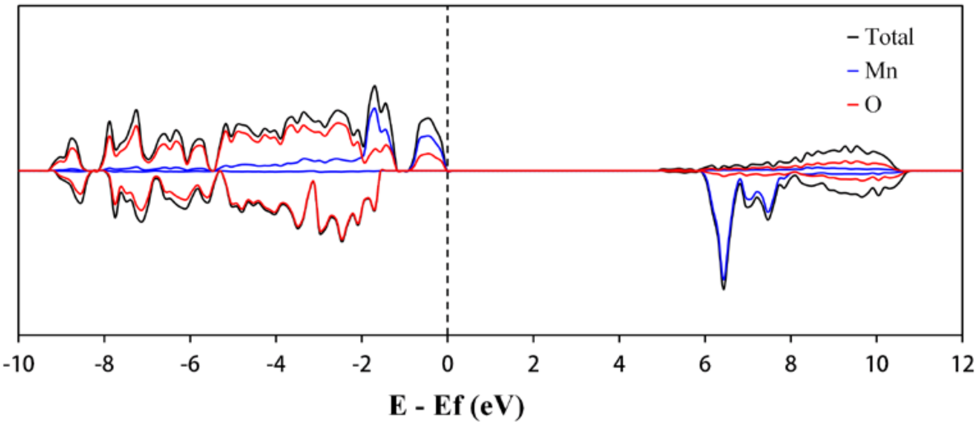

Figure S3. The total density of states (DOS) and local DOS of Mn and O components for $Na_2MnP_2O_7$. The HSE06 screened hybrid functional was used for calculation.